

Provided for non-commercial research and education use.  
Not for reproduction, distribution or commercial use.



This article appeared in a journal published by Elsevier. The attached copy is furnished to the author for internal non-commercial research and education use, including for instruction at the authors institution and sharing with colleagues.

Other uses, including reproduction and distribution, or selling or licensing copies, or posting to personal, institutional or third party websites are prohibited.

In most cases authors are permitted to post their version of the article (e.g. in Word or Tex form) to their personal website or institutional repository. Authors requiring further information regarding Elsevier's archiving and manuscript policies are encouraged to visit:

<http://www.elsevier.com/authorsrights>



Contents lists available at SciVerse ScienceDirect

## Journal of Alloys and Compounds

journal homepage: [www.elsevier.com/locate/jalcom](http://www.elsevier.com/locate/jalcom)

# Electrical properties of fast ion conducting silver based borate glasses: Application in solid battery



Emad M. Masoud\*, M. Khairy, M.A. Mousa

Chemistry department, Faculty of Science, Benha University, Benha, Egypt

## ARTICLE INFO

## Article history:

Received 7 January 2013

Received in revised form 5 March 2013

Accepted 11 March 2013

Available online 26 March 2013

## Keywords:

Silver ionic glasses

Electrical conductivity

Dielectric constant

Silver iodine battery

## ABSTRACT

The electrical properties of the ternary ionic conducting glass system  $x\text{AgI}-(1-x)[0.67\text{Ag}_2\text{O}-0.33\text{B}_2\text{O}_3]$ , where  $x = 0.4, 0.5, 0.6, 0.7$  and  $0.8$ , were studied for emphasizing the influence of silver iodide concentration on the transport properties in the based borate glasses. The glasses were prepared by melt quenching technique and characterized using X-ray diffraction (XRD), FT-IR spectra and differential thermal analysis (DTA). XRD confirmed a glassy nature for all investigated compositions. Electrical conductivity ( $\sigma$ ), dielectric constant ( $\epsilon'$ ), dielectric loss ( $\epsilon''$ ) and impedance spectra ( $Z'-Z''$ ) were studied for all samples at a frequency range of  $0-10^6$  Hz and over a temperature range of  $303-413$  K. Changes of conductivity and dielectric properties with composition, temperature and frequency were analyzed and discussed. A silver iodine battery using glassy electrolyte sample with the highest ionic conductivity ( $x = 0.6$ ) was studied.

© 2013 Elsevier B.V. All rights reserved.

## 1. Introduction

The understanding of ion diffusion process in super ionic glasses is of both practical and academic interest. These materials are currently under investigation for technical application as solid electrolytes in electrochemical devices such as batteries, sensors and electrochromic displays. due to their high ionic conductivity, high stability and large available composition ranges [1]. It is also interesting in the academic level to understand the nature of ion diffusion in these materials. Many oxide glasses consisting of different glass former ( $\text{B}_2\text{O}_3$ ,  $\text{P}_2\text{O}_5$ ,  $\text{V}_2\text{O}_5$ ,  $\text{AgPO}_3$ ,  $\text{TeO}_2$ ,  $\text{Bi}_2\text{O}_3$ ,  $\text{MoO}_3$  and others), a metal oxide  $\text{M}_2\text{O}$  ( $\text{M} = \text{Ag}, \text{Li}, \text{Na}$  and  $\text{K}$ ) and a doping salt  $\text{MX}$  ( $\text{X} = \text{I}, \text{Cl}, \text{Br}$  and  $\text{F}$ ) were investigated [2–8].

A particularly interesting class of fast ion conductors is the AgI-doped silver borate glasses [1]. Several attempts were performed using different methods to modify and improve the ionic conductivity ( $\sigma_i$ ) of silver borate glasses. One of these methods is the dopant concentration change to produce high ionic conductivity at a definite concentration of doping materials. In the present work, we study the influence of AgI concentration upon silver ion conduction in the glass system of  $\text{AgI}-\text{Ag}_2\text{O}-\text{B}_2\text{O}_3$ . Application of these glasses as solid electrolytes in solid batteries is one of our targets.

## 2. Experimental

Glass samples with a general formula of  $x\text{AgI}-(1-x)[0.67\text{Ag}_2\text{O}-0.33\text{B}_2\text{O}_3]$ , where  $x = 0.4, 0.5, 0.6, 0.7$  and  $0.8$  were prepared by melt quenching technique. Stoichiometric quantities of silver iodide, silver oxide and boron oxide were used to get the required composition then mixed and ground to obtain a homogeneous mixture. The mixtures were melted at  $1223$  K in a porcelain crucible for  $30$  min and then rapidly quenched onto a stainless steel plate maintained at room temperature. All samples were characterized using X-ray diffraction by means of a Phillips X-ray diffractometer (Model PW 1710).

Differential thermal analysis (DTA) was performed in a static air atmosphere with a constant heating rate of  $10$  K/min in a temperature range of  $298-873$  K using Shimadzu DT-50. FT-IR spectra were recorded using KBr pellet technique on IR-Brucker, Vector 22, Germany. Electrical measurements were carried out for samples with thickness of  $\sim 1$  mm using two probe method at a constant voltage ( $1$  V) using a programmable automatic LCR bridge (model RM 6306 Phillips bridge). The measurements were performed over a temperature range of  $303-413$  K and frequencies between  $0$  and  $10^6$  Hz.

## 3. Results and discussion

XRD spectra of  $x\text{AgI}-(1-x)[0.67\text{Ag}_2\text{O}-0.33\text{B}_2\text{O}_3]$ , where  $x = 0.4, 0.5$  and  $0.6$ , showed amorphous nature, Fig. 1, and confirmed that these samples are glassy in nature. Samples with a composition of  $x = 0.7$  and  $0.8$  showed an amorphous structure with some patterns characteristic to  $\alpha$  and  $\beta$ -AgI crystals [1].

The main IR-bands of investigated glasses, Table 1, showed vibration bands characteristic for the presence of  $\text{BO}_3$  and  $\text{BO}_4$  groups and B–O bonds in borate triangles found in glasses below the meta borate stoichiometry [9]. A band at a range of  $900-874$   $\text{cm}^{-1}$  is also observed in all glasses and assigned to the bending of B–O–B linkages in the borate networks. Generally, the

\* Corresponding author. Address: Chemistry Department, Faculty of Science, Benha University 13518 Benha, Qalioubya Governorate, Egypt. Tel.: +20 002 01203532343.

E-mail address: [emad\\_masoud1981@yahoo.com](mailto:emad_masoud1981@yahoo.com) (E.M. Masoud).

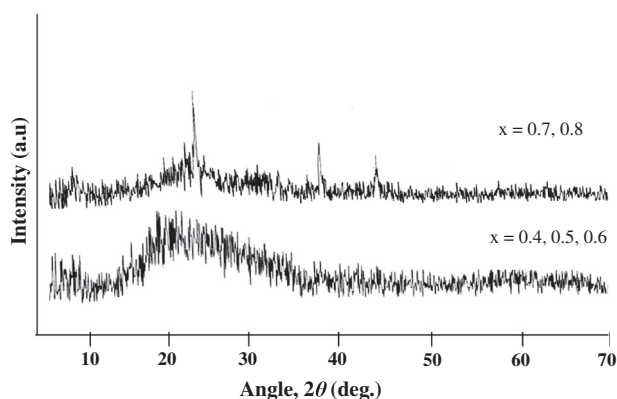


Fig. 1. XRD for  $x\text{AgI}-(1-x)[0.67\text{Ag}_2\text{O}-0.33\text{B}_2\text{O}_3]$ , where  $x = 0.4, 0.5, 0.6, 0.7$  and  $0.8$ .

observed shifts of the main bands referred to affecting the glass structure with composition change. Thermal analyses showed DTA-thermograms with endothermic peaks observed between 360 and 377 K for samples with a composition of  $x > 0.6$  due to the  $\beta \rightarrow \alpha$  AgI phase transition [1], Table 2. The thermograms show also a glass transition temperature ( $T_g$ ) for each sample followed by an endothermic peak due to melting of the glass.  $T_g$  decreased with AgI increasing. This refers to that the glass becomes more soften and the glass network becomes more opened with increasing the amount of AgI in the samples.

Density and molar volume values of the glassy system changed with AgI concentration, Table 2. The change of molar volume shows an opposite trend to that observed for the density behavior. This behavior refers to a formation of more opened network glass with AgI increasing. This trend goes in parallel way with decreasing the intensities of  $\text{B}-\text{O}^-$  and  $\text{BO}_4^-$  bands observed in IR-spectra.

The temperature dependence of dc-conductivity ( $\sigma_{dc}$ ) for the glassy system has been studied over a temperature range between 303 and 413 K. The plots of  $\ln \sigma_{dc}$  vs.  $1/T$ , for all samples, show a continuous increasing of conductivity with temperature. The sample with  $x = 0.8$  shows a kink in the temperature dependence curve, Fig. 2. For all temperature ranges, a semiconducting behavior is observed and characterized by Arrhenius dependence

$$\sigma_{dc} = \sigma_0 \exp(-E_{dc}/kT) \quad (1)$$

where  $\sigma_0$  is a constant,  $E_{dc}$  is the activation energy,  $k$  is the Boltzmann constant and  $T$  is the absolute temperature. The conductivity

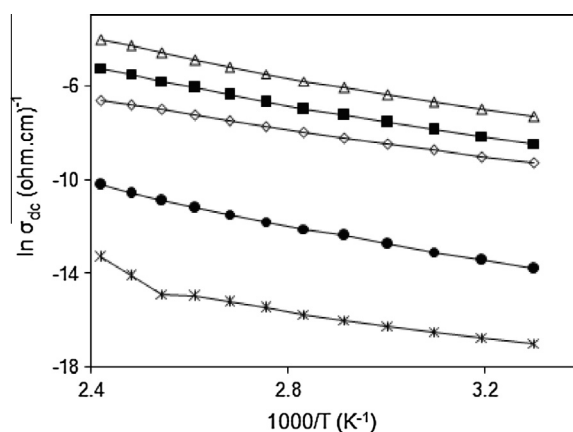


Fig. 2. Temperature dependence of dc-conductivity for investigated glassy samples:  $\diamond$ ,  $\blacksquare$ ,  $\triangle$ ,  $\bullet$  and  $*$  for samples with  $x = 0.4, 0.5, 0.6, 0.7$  and  $0.8$  respectively.

data are calculated and listed in Table 3. The composition dependence of dc-conductivity value at room temperature ( $\sigma_{dc}$ ) changes according to the following order:

$$\sigma_{dc}(x = 0.6) > \sigma_{dc}(x = 0.5) > \sigma_{dc}(x = 0.4) > \sigma_{dc}(x = 0.7) > \sigma_{dc}(x = 0.8)$$

This trend goes in a parallel way with molar volume increase, which causes an easily motion of silver ions (charge carriers) within the glass matrix.

The mobility of charge carriers ( $\mu$  in the glassy samples is calculated from:

$$\sigma_{dc} = ne\mu \quad (2)$$

where  $n$  is the charge carrier concentration and  $e$  is the electronic charge. The results obtained are listed in Table 3 and showed that density of charge carriers ( $n$ ) changes with concentration of AgI by factor of  $\sim 2.5$ , whereas the mobility changes by factor of  $\sim 3.4 \times 10^4$ . This means that AgI not only supplies mobile  $\text{Ag}^+$  ions but also facilitates their motion in the  $\text{I}^-$  containing environment. Such environment, in which stronger covalent bonding is replaced by a weaker ionic one is a decisive factor of high ionic conductivity of the best silver ion conductors like  $\alpha\text{-AgI}$  [10]. The activation of dc-conductivity ( $\sigma_{dc}$ ) with temperature increasing can be interpreted by the Minami structure model [11]. This model suggested

Table 1  
Main IR-bands in the glass system  $x\text{AgI}-(1-x)[0.67\text{Ag}_2\text{O}-0.33\text{B}_2\text{O}_3]$ , [ $x = 0.4, 0.5, 0.6, 0.7$  and  $0.8$ ].

| Structural groups and chemical bonds                | Wave number ( $\text{cm}^{-1}$ ) |      |      |      |      |
|---|----------------------------------|------|------|------|------|
|   | 0.4                              | 0.5  | 0.6  | 0.7  | 0.8  |
| Vibration of $\text{BO}_3$ group                    | 720                              | 715  | 710  | 703  | 701  |
| Vibration of $\text{BO}_4^-$                        | 855                              | 845  | 841  | 838  | 836  |
| B-O-B bending                                       | 900                              | 897  | 891  | 888  | 874  |
| Vibration of B-O network                            | 1027                             | 1021 | 1018 | 1013 | 1004 |
| B-O stretching vibration of $\text{BO}_3$           | 1320                             | 1327 | 1321 | 1329 | 1332 |
| $\text{BO}_3$ stretching vibration Of B-O-B network | 1376                             | 1371 | 1374 | 1369 | 1361 |

Table 2  
Thermal and density data for the glass system  $x\text{AgI}-(1-x)[0.67\text{Ag}_2\text{O}-0.33\text{B}_2\text{O}_3]$ , [ $x = 0.4, 0.5, 0.6, 0.7$  and  $0.8$ ].

| $x$ (Ag I) | $\beta \rightarrow \alpha$ transition (K) | $T_g$ (K) | $T_m$ (K) | Density ( $\text{g}/\text{cm}^3$ ) | Molar volume ( $\text{cm}^3/\text{mol}$ ) |
|------------|---|-----------|-----------|------------------------------------|---|
| 0.4        | -   | 491       | 536       | 6.25                               | 32.1                                      |
| 0.5        | -   | 470       | 516       | 6.19                               | 33.3                                      |
| 0.6        | -   | 430       | 489       | 6.21                               | 34.1                                      |
| 0.7        | 377                                       | 425       | 470       | 7.02                               | 31.0                                      |
| 0.8        | 360                                       | 420       | 452       | 7.32                               | 30.5                                      |

**Table 3**  
Conductivity data for glass system:  $x\text{AgI}-(1-x)[0.67\text{Ag}_2\text{O}-0.33\text{B}_2\text{O}_3]$ , [ $x = 0.4, 0.5, 0.6, 0.7$  and  $0.8$ ].

| $x(\text{AgI})$ | Temp. range (K) | $E_{dc}$ (eV) | $\sigma_{dc} \times 10^4 (\Omega^{-1} \text{cm}^{-1})$ | $\sigma_b \times 10^5 (\Omega^{-1} \text{cm}^{-1})$ | $n \times 10^{-21} (\text{cm}^3)$ | $\mu (\text{cm}^2 \text{V}^2 \text{s}^{-1})$ |
|-----------------|-----------------|---------------|--|---|-----------------------------------|--|
| 0.4             | 303–413         | 0.29          | 0.91   | 1.12  | 4.05                              | $1.4 \times 10^{-7}$                         |
| 0.5             | 303–413         | 0.32          | 2.11   | 4.12  | 2.61                              | $5.1 \times 10^{-7}$                         |
| 0.6             | 303–413         | 0.31          | 6.73   | 9.21  | 1.88                              | $2.2 \times 10^{-6}$                         |
| 0.7             | 303–413         | 0.35          | $1.01 \times 10^{-2}$                                  | $5.0 \times 10^{-2}$                                | 2.1                               | $3.1 \times 10^{-9}$                         |
| 0.8             | 303–393         | 0.24          | $4.14 \times 10^{-4}$                                  | $7.0 \times 10^{-3}$                                | 4.07                              | $6.4 \times 10^{-11}$                        |
|                 | 393–413         | 1.12          |  |   |                                   |  |

$\sigma_{dc}$ ;  $\sigma_b$ ;  $n$  and  $\mu$  are calculated at 303 K.

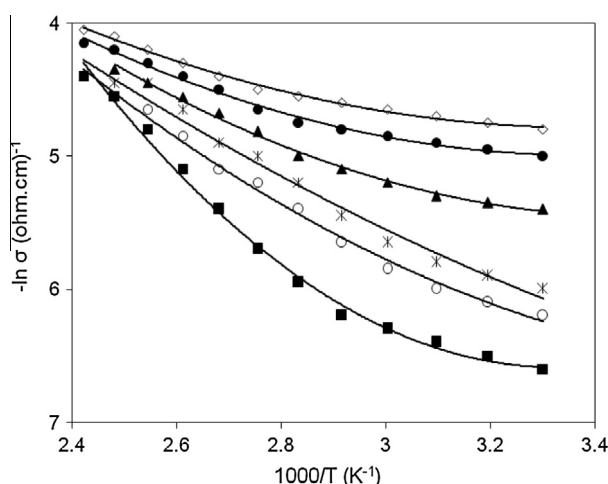


**Fig. 3.** Effect of temperature on ac-electrical conductivity of  $(\text{AgI})_{0.5}[0.67\text{Ag}_2\text{O}-0.33\text{B}_2\text{O}_3]_{0.5}$ ;  $\blacksquare, \circ, *, \blacktriangle, \bullet$  and  $\diamond$  for  $5 \times 10^4, 1 \times 10^5, 2.5 \times 10^5, 5 \times 10^5, 7 \times 10^5$  and  $1 \times 10^6$  Hz, respectively.

the occurrence of three  $\text{Ag}^+$  ions with different mobility (i)  $\text{Ag}^+$  ions bonded to the oxygen atoms of the network, (ii)  $\text{Ag}^+$  ions interact weakly with the network oxygen atoms, (iii)  $\text{Ag}^+$  ions surrounded by  $\text{I}^-$  ions only. Silver ions of the last type have a maximum mobility and contribute mostly to an ionic conduction. When the temperature increases,  $\text{Ag}^+$  ions (which interact weakly to the oxygen atoms of the network) may release and contribute in conduction with  $\text{Ag}^+$  ions, which surrounded by  $\text{I}^-$  ions, and this will lead to increase the concentration of mobile  $\text{Ag}^+$  ions.

The ac-conductivity ( $\sigma_{ac}$ ), dielectric constant ( $\epsilon'$ ), dielectric loss ( $\epsilon''$ ) and complex impedance ( $Z^*$ ) were studied for the glassy system at a temperature range of 303–413 K and frequencies between  $10^2$  and  $10^6$  Hz.

The effect of temperature on the ac-conductivity ( $\ln \sigma_{ac}$  vs.  $1/T$ ) shows a behavior in which  $\sigma_{ac}$  increases with temperature increasing. Typical plots are represented in Fig. 3. The ac-conductivity data of the investigated system comply to a large extent with the following equation:

$$\sigma_{ac} = \sigma_0 \exp(-E_{ac}/kT) \quad (3)$$

where  $E_{ac}$  represents the activation energy of the conduction mechanism. The values of  $E_{ac}$ , over a different range of temperature, were calculated at different frequencies for each composition. The conductivity data are listed in Table 4.

The temperature influence of ac-conductivity has been explained by considering the mobility of charge carriers is responsible for hopping. As a temperature increases, the mobility of hopping ions also increases and thereby contributing in conductivity increase [12]. It is known that, for the dc-conductivity, the charge carriers choose the easiest path between the ions. These

**Table 4**  
Ac-conductivity data for glass system:  $x\text{AgI}-(1-x)[0.67\text{Ag}_2\text{O}-0.33\text{B}_2\text{O}_3]$ , [ $x = 0.4, 0.5, 0.6, 0.7$  and  $0.8$ ].

| $x(\text{AgI})$ | Temperature range (K) | $E_{ac}$ (eV) |         |          | $W_m$ (eV) |
|-----------------|-----------------------|---------------|---------|----------|------------|
|                 |                       | 50 kHz        | 500 kHz | 1000 kHz |            |
| 0.4             | 303–353               | 0.26          | 0.25    | 0.24     | 0.36       |
|                 | 363–413               | 0.13          | 0.14    | 0.14     | 0.36       |
| 0.5             | 303–363               | 0.25          | 0.25    | 0.23     | 0.38       |
|                 | 373–413               | 0.12          | 0.12    | 0.12     | 0.38       |
| 0.6             | 303–413               | 0.18          | 0.09    | 0.13     | 0.41       |
| 0.7             | 303–413               | 0.17          | 0.10    | 0.11     | 0.44       |
| 0.8             | 303–323               | 0.14          | 0.13    | 0.14     | 0.21       |
|                 | 333–373               | 0.03          | 0.003   | 0.02     | 0.76       |
|                 | 383–413               | 1.70          | 1.50    | 1.60     | 0.08       |

paths will include some jumps for which  $R$ , the distance between the ions, is large. This is not so important in the ac-conduction which in turn lowers the activation energy for conduction process. The difference between activation energies of  $\sigma_{dc}$  and  $\sigma_{ac}$  may be also attributed to the effective drop of the electric field within the bulk due to the presence of space charge accumulations at the electrodes in dc-measurements [13].

Fig. 4 shows a typical ac-conductivity behavior at different temperatures. The sample exhibited the high frequency dispersion and a frequency-independent conductivity at low frequencies. The frequency dispersion of the conductivity is due to the fact that inhomogeneities in the glasses may be of a microscopic in nature with the distribution of relaxation processes through distribution of energy barriers [14].

The dependence of  $\sigma_{ac}$  upon  $\omega$  can be estimated at different temperatures according to equation [15]:

$$\sigma_{ac} = A\omega^s \quad (4)$$

The behavior of  $s$  with temperature can be taken as a criterion of the conduction mechanism [15,16]. For all samples, our results show that the exponent  $s$  values lie in the range of 0.1–0.7 and decrease with increasing the temperature referring to a translational hopping motion. The results can be also explained according to the unified site relaxation model and diffusion controlled relaxation (DCR) models [17,18]. The variation of  $s$  as a function of temperature can be directly related to the existence of a range of relaxation processes and an ion diffusion mechanism in the glass matrix and the magnitude of  $s$  contributes to the measured ac-conductivity.

The temperature and frequency dependence of dielectric constant ( $\epsilon'$ ) shows a similar trend for all investigated compositions, typical plot is shown in Fig. 5. It shows that dispersion of dielectric constant is high at lower frequencies. This is because when an electrical stimulus is applied, the flow of charge carriers agglomerates across the electrode–electrolyte interface creating space charge layers. This leads to a high value of a capacitance at the interfaces, which decreases with frequency increasing. The low frequency

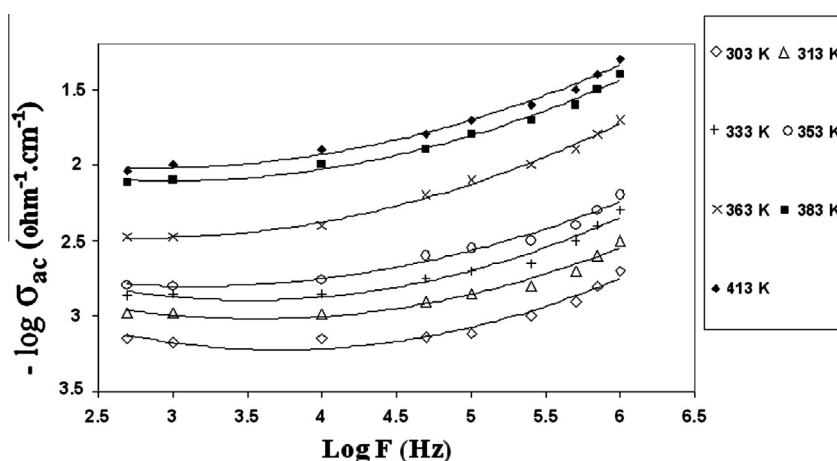


Fig. 4. Effect of frequency on ac-electrical conductivity of  $(AgI)_{0.5}[0.67Ag_2O-0.33B_2O_3]_{0.5}$  at different temperatures.

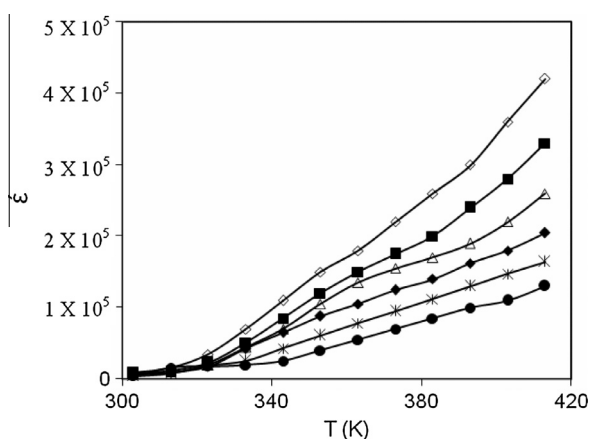


Fig. 5. Effect of temperature and frequency on dielectric constant of  $(AgI)_{0.5}[0.67Ag_2O-0.33B_2O_3]_{0.5}$ ,  $\diamond$ ,  $\blacksquare$ ,  $\triangle$ ,  $\blacklozenge$ ,  $+$  and  $\bullet$  for  $5 \times 10^4$ ,  $1 \times 10^5$ ,  $2.5 \times 10^5$ ,  $5 \times 10^5$ ,  $7 \times 10^5$  and  $1 \times 10^6$  Hz, respectively.

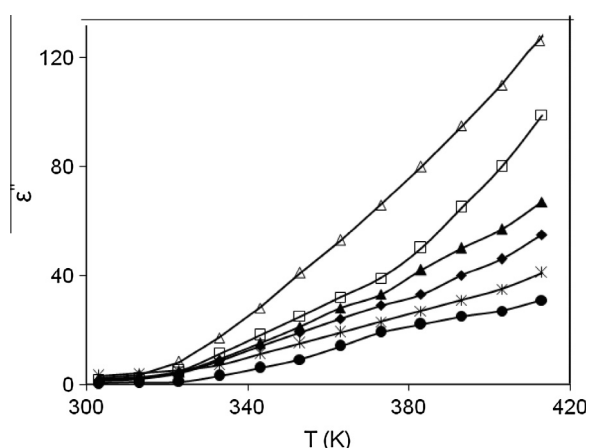


Fig. 6. Effect of temperature and frequency on dielectric loss for  $(AgI)_{0.5}[0.67Ag_2O-0.33B_2O_3]_{0.5}$ ,  $\diamond$ ,  $\square$ ,  $\triangle$ ,  $\blacklozenge$ ,  $+$  and  $\bullet$  for  $5 \times 10^4$ ,  $1 \times 10^5$ ,  $2.5 \times 10^5$ ,  $5 \times 10^5$ ,  $7 \times 10^5$  and  $1 \times 10^6$  Hz, respectively.

dispersion (LFD, at high frequencies) behavior is related to the extended motion of charge carriers and may be associated with either volume or interfacial phenomena [19]. It may be possible to distinguish between the two mechanisms such as volume and interfacial

processes. In general, if the real part ( $\epsilon'$ ) and the imaginary part ( $\epsilon''$ ) remain parallel over a large frequency range, then LFD can be associated to a volume process, otherwise it corresponds to an interfacial process [20]. In our system,  $\epsilon'$  deviates to a great extent with frequency, Fig. 5, which corresponds to an interfacial process. Generally, the high value of dielectric constant at low frequencies is attributed to the interfacial ionic polarizations due to localized  $Ag^+$  ion motion within the glass network [21].

The temperature dependence of  $\epsilon'$  shows an increase of  $\epsilon'$ -value with temperature increase, Fig. 5. As with raising temperature, the glass network relaxes and the ionic motion becomes more easily. The increase of ( $\epsilon'$ ) is more pronounced at low frequency range, because the ions have more time to participate in the motion.

The change of dielectric loss ( $\epsilon''$ ) with frequency at different temperatures is shown in Fig. 6. The variation in  $\epsilon''$  with frequency is large at higher temperatures. The experimental results of  $\epsilon''$  obtained in the present study can be explained by Stevel's model [22]. According to this model, the conductivity in the solid electrolyte is visualized as a series of jumps by ions along the lattice sites. If all sites are equivalent, the ions spend equal amount of time at each site during the conduction process. This is not the case when the sites are not equal. Thus, the charge carriers tend to pile up at high free energy barriers resulting in an increase of capacitance at low frequency. Therefore, the variation of  $\epsilon''$  at lower frequencies is due to the long range diffusion of  $Ag^+$  ions involving a series of jumps over barriers of varying height. At higher frequencies, the periodic reversal of field takes place so rapidly that there are no excess ionic jumps in the field direction. It can be observed that dielectric loss increases with temperature due to the orientation of dipoles which facilitate the increase of permittivity at higher temperatures [23,24].

The temperature dependence of dielectric loss at fixed frequencies for the glassy system shows that dielectric loss ( $\epsilon''$ ) increases with temperature, Fig. 6. The decrease in dielectric loss value with increasing the frequency can be attributed to the decrease in the diffusion rate of silver ions in the glass matrix with frequency increasing. Consequently, there is a phase lag between the applied field and the polarization of the glass. This, in turn, leads to an energy absorbed from the electric field to the dielectric material.

The dielectric loss can be expressed as [25]:

$$\epsilon'' = A\omega^m \tag{5}$$

where  $m = -4kT/W_m$ . The values of  $A$ ,  $m$  and activation energy ( $W_m$ ) are obtained using least squares fitting and given in Table 4. The obtained values of  $W_m$  are higher than the activation energies obtained using dc-conductivity for all samples except for  $x = 0.8$ .

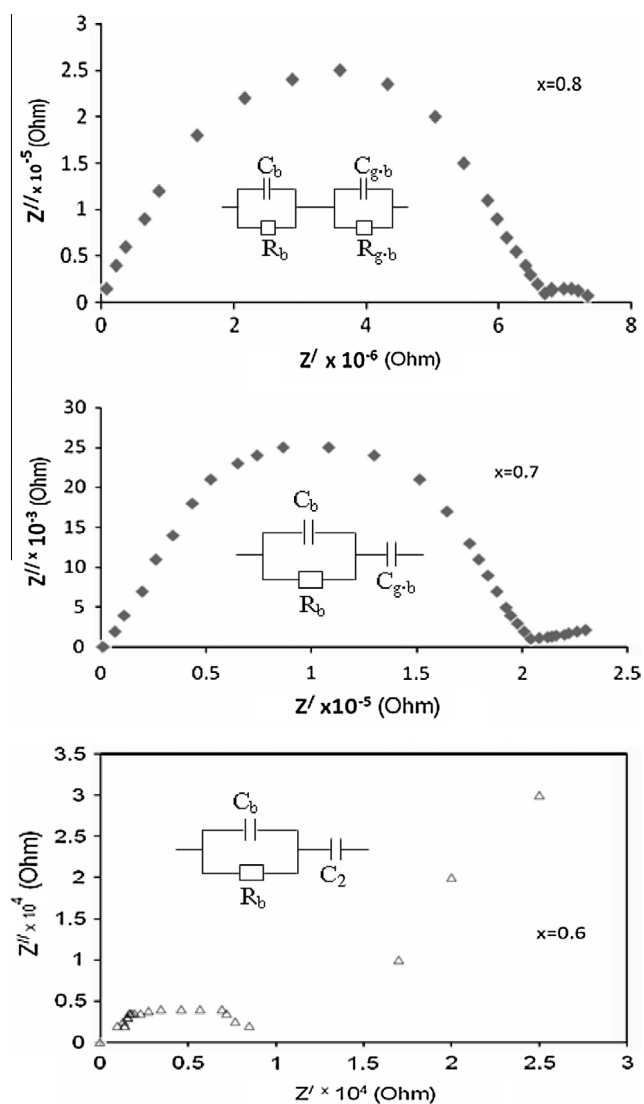


Fig. 7. Impedance spectra at 323 K for glassy samples with  $x = 0.6, 0.7$  and  $0.8$ .

This can be attributed to the contribution of some localized defects present in the glass system in the relaxation process.

The complex impedance analysis method was also used to test the effect of glass composition on type of conduction. The impedance was measured at 303 K over a frequency range of  $10^2$ – $10^6$  Hz and analyzed to a real part ( $Z'$ ) and imaginary part ( $Z''$ ) on the complex plane, Fig. 7. The impedance spectrum exhibits a behavior depends on composition of the sample. The spectra for samples with  $x = 0.4$ – $0.6$  consist of high frequency semicircles and low frequency spur, which exhibits some bending. This refers to the behavior predominates for ionic conducting transport. The formation of the inclined straight line at the low frequency region represents the capacitance effect at the electrode and electrolyte interface, and this is called the double layer capacitance effect. The impedance spectrum for the sample with a composition of  $x = 0.7$  exhibits a semicircle at high frequencies with tail at low frequency side. The tail represents Warburg impedance and comes from a distribution of relaxation times in the sample as a result of inhomogeneity in the glassy sample. On the other hand, the impedance spectrum for the sample with a composition of  $x = 0.8$  consists of a large semicircle at high frequencies followed with a second small one at low frequency end, representing the bulk and grain boundary responses to the applied voltage. The

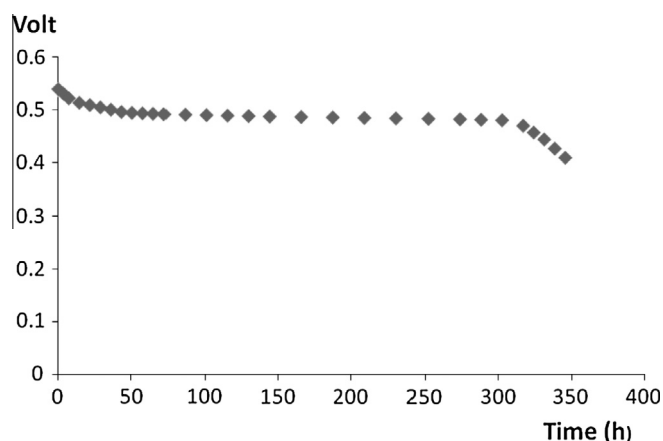


Fig. 8. Discharge characteristic for solid cell using  $0.6\text{AgI}-0.4 [0.67\text{Ag}_2\text{O}-0.33\text{B}_2\text{O}_3]$  glassy electrolyte ( $T = 303$  K, current density  $10 \mu\text{A}/\text{cm}^2$ ).

equivalent circuit of each glass has been suggested and given also in Fig. 7. The bulk conductivity value ( $\sigma_b$ ) obtained are listed in Table 3. It shows that  $\sigma_b$ -values change with the composition in the same order of that obtained from dc-measurements.

A charge–discharge characteristic of solid state cell consists of Ag powder + electrolyte/electrolyte/ $\text{I}_2$  + C + electrolyte has been studied. The glassy electrolyte used is  $0.6\text{AgI}-0.4 [0.67\text{Ag}_2\text{O}-0.33\text{B}_2\text{O}_3]$ , which exhibits the highest ionic conductivity in our samples. The assembly cell had an effective area of  $0.25 \text{ cm}^2$ , thickness of  $0.22 \text{ cm}$  and weight of  $1.3 \text{ g}$ . The anode was made of 67 wt.% glass and 33 wt.% silver powder. The composition of cathode was 30 wt.% carbon and 70 wt.% iodine. Anode, electrolyte and cathode were pressed together under  $4.5 \text{ ton}/\text{cm}^2$ . The discharge curve is shown in Fig. 8. It corresponds to a load resistance of  $45 \text{ k Ohm}$  and a current density of  $10 \mu\text{A}/\text{cm}^2$ . The plateau of the discharge curve is  $0.51 \text{ V}$ . Under comparable discharge conditions, the life time of the battery using the glass electrolyte is 20% less than with  $\text{RbAg}_4\text{I}_5$  (320 against 400 h) [26].

## 5. Conclusions

Ternary ionic conducting glass system with a composition of  $x\text{AgI}-(1-x)[0.67\text{Ag}_2\text{O}-0.33\text{B}_2\text{O}_3]$ , where  $x = 0.4, 0.5, 0.6, 0.7$  and  $0.8$  was prepared using melt-quenching technique. The glass transition temperature ( $T_g$ ) changes with silver iodide concentration increasing reflecting the formation of the most opened network structure at  $x = 0.6$ . The conductivity of the glassy system was found to depend on concentration of dopant AgI. The sample with a composition of  $x = 0.6$  showed the highest value of dc-conductivity ( $\sigma_{dc} = 6.73 \times 10^{-4} \Omega^{-1} \text{ cm}^{-1}$ , at 303 K). The dc-electrical conductivities ( $\sigma_{dc}$ ) for borate system increase according to:  $\sigma_{dc} (x = 0.6) > \sigma_{dc} (x = 0.5) > \sigma_{dc} (x = 0.4) > \sigma_{dc} (x = 0.7) > \sigma_{dc} (x = 0.8)$ . The bulk conductivities showed a parallel matching with values of  $\sigma_{dc}$  at 303 K. Values of dielectric constant and dielectric loss change markedly with silver iodide concentration. Study of charging and discharging of the solid electrolyte showed that it is possible to use borate system with  $x = 0.6$  as a solid electrolyte in solid battery.

## References

- [1] S. Bhattacharya, A. Ghosh, Chem. Phys. Lett. 424 (2006) 295.
- [2] D. Dutta, A. AGhosh, Phys. Rev. B 72 (2005) 024201.
- [3] P. Kumar, S. Yashonath, J. Chem. Sci. 118 (2006) 135.
- [4] M.G. El-Shaarawy, W.A. Bayoumy, J. Phys. Soc. Jpn 77 (2004) 2017.
- [5] E. Barsoukov, J.R. Macdonald, Impedance Spectroscopy, Wiley-Interscience, 2nd Ed. (2005).

- [6] R.C. Agrawal, A. Chandra, A. Bhatt, Y.K. Mahipal, *J. Phys. D.: Appl. Phys.* 40 (2007) 4714.
- [7] S. Bhattacharya, A. Ghosh, *Phys. Rev. B* 70 (2004) 72203.
- [8] A. Dutta, A. Ghosh, *J. Non-cryst. Solids* 351 (2005) 203.
- [9] R.C. Agrawal, R. Kumar, *J. Phys. D. Appl. Phys.* 27 (1994) 2432.
- [10] S. Chandra, *Superionic Solids*, North-Holland Publ. Co., 1981.
- [11] T. Minami, *J. Non-Cryst. Sol.* 56 (1983) 15.
- [12] H. Scholze, *Glass-Nature, Structure and Properties*, Springer, New York, 1991.
- [13] S.R. Elliott, *Solid State Ionics* 27 (1988) 131.
- [14] R. Murugaraj, G. Govindaraj, D. George, *Matter. Lett.* 57 (2003) 1656.
- [15] M. Pollak, Y.H. Gaballe, *Phys. Rev.* 122 (1961) 1742.
- [16] D.A. Keen, R.L. Mc Greevy, *Nature* 344 (1990) 423.
- [17] K.L. Ngai, *J. Non, Cryst. Sol.* 203 (1996) 232.
- [18] N.K. Karan, B. Natesan, R.S. Katiyar, *Solid State Ionics* 177 (2006) 1429.
- [19] A. Bunde, P. Maass, *J. Non-Cryst. Sol.* 131 (1991) 1022.
- [20] A. Rivera, J. Santamaria, C. Leon, T. Blochowicz, C. Gainaru, E.A. Roseler, *Appl. Phys. Lett.* 82 (2003) 2425.
- [21] B.V.R. Chowdari, K. Radhakrishnan, *J. Non-Cryst. Sol.* 110 (1989) 101.
- [22] K.P. Padmasereek, K. Kanchand, *Mater. Chem. Phys.* 91 (2005) 551.
- [23] Tareev, *Physics of Dielectric Materials*, Mir Publishers, Moscow, 1975.
- [24] S. Selvasekarapandian, R. Chitra Devi, M. Vijaya Kumar, in: B.V.R. Chowdari et al. (Eds.), *Solid State Ionic Materials and Devices*, World Scientific, Singapore, 2000.
- [25] J.C. Giuntini, J.V. Zanchetta, D. Jullien, R. Eholie, Houenou, *J. Non-Cryst. Sol.* 45 (1981) 57.
- [26] L. Tu Jun, J. Portier, B. Tanguy, J.J. Videau, M. Ait Allal, J. Morcos, J. Salardenne, *Active and Passive Electron. Comp.* 14 (1990) 8.